Accurate calculation of spin-state energy gaps in Fe(III) Spin-Crossover systems using Density Functional Methods

Daniel Vidal[1,2], *Jordi Cirera*[1] * *and Jordi Ribas-Arino*[2] *

[1] Departament de Química Inorgànica i Orgànica and Institut de Recerca de Química Teòrica i Computacional, Universitat de Barcelona, Diagonal 645, 08028 Barcelona, Spain

[2] Departament de Ciència de Materials i Química Física and Institut de Recerca de Química Teòrica i Computacional, Universitat de Barcelona, Diagonal 645, 08028 Barcelona, Spain

e-mail: j.ribas@ub.edu
e-mail: jordi.cirera@qi.ub.es

Abstract

Fe(III) complexes are receiving ever-increasing attention as spin crossover (SCO) systems because they are usually air stable, as opposed to Fe(II) complexes, which are prone to oxidation. Here, we present the first systematic study exclusively devoted to assess the accuracy of several exchange-correlation functionals when it comes to predicting the energy gap between the high-spin (S=5/2) and the low-spin (S=1/2) states of Fe(III) complexes. Using a dataset of 24 different Fe(III) hexacoordinated complexes, it is demonstrated that the B3LYP* functional is an excellent choice not

only for predicting spin-state energy gaps for Fe(III) complexes undergoing spin-transitions but also for discriminating Fe(III) complexes that are either low- or high-spin in the whole range of temperatures. Our benchmark study has led to the identification of a very versatile Fe(III) compound whose SCO properties can be engineered upon changing a single axial ligand. Overall, this work demonstrates that B3LYP* is a reliable functional for screening new spin-crossover systems with tailored properties.

Keywords: Spin-Crossover, Density Functional Theory, Electronic Structure, Iron(III) complexes

1. Introduction

Switchable molecules and materials are key elements in the design of the new generation of nanodevices due to their inherent bi-stable behavior. Among them, spin-crossover (SCO) systems, molecules and materials that have access to two alternative electronic states close in energy, are particularly interesting due to their flexibility in design and tunability.[1–18] In SCO systems, the spin-state manipulation can be done using an external stimulus, usually temperature, but can be also induced by means of pressure or electromagnetic radiation. The thermal transition, which is by far the most common one, takes place when the entropic term overcomes the enthalpic one, shifting the system from the low-spin state to the high-spin one.[19,20] The temperature with equal populations of both spin-states is defined as the transition temperature ($T_{1/2}$), and this is a key parameter in the physical characterization of the system. Since their discovery by Cambi and co-workers in 1931,[21] SCO systems have been the focus of attention of many researchers due to their potential and practical application as

molecular level switches.[4,5,7,9,14,22] Much development has been done in the field over the last decades, expanding the number of metal centers and coordination environments able to exhibit such behavior. As much experimental information as there is, the rational design of new SCO systems with tailored properties relies heavily on the experience. For that reason, the vast majority of newly reported SCO systems build upon the Fe^{II}-hexacoordinated motif with six nitrogen donor atoms.[23–31] However, d^6-Fe(II) SCO complexes are air unstable, and tend to oxidize and lose their switching behavior, which makes its application in actual devices challenging. For that reason, there is an increasing interest in the design of new SCO systems with d^5-Fe(III) metal centers,[31–35] systems that exhibit a much larger stability towards oxidation and, therefore, show more potential towards its use in technological devices. In the case of Fe(III) centers, the high-spin (HS) and low-spin (LS) states involved in the spin transition are commonly a sextet spin state (S=5/2) and a doublet spin state (S=1/2), respectively. Despite the increasing interest in such systems,[31–35] which has been recently reviewed, there is less experimental information and, therefore, the rational design of new Fe(III)-SCO systems with tailored properties becomes challenging. In particular, designing a molecule with a given transition temperature is extremely difficult. In that sense, great progress has been done in the field of computational modelling of SCO systems, and some methodologies have been presented aiming to reproduce the behavior of such systems, and even their intersystem crossing rates.[20,36–62] In particular, much development has been done over the last years in the modelling of $T_{1/2}$ for several families of SCO systems,[63–68] including the study of spin-state energy gaps in Fe(III) systems.[45] Motivated by such results, we decided to explore the potential use of such methods to quantitatively calculate $T_{1/2}$ in Fe(III)-SCO systems. In this work, several DFT methods have been

used towards a dataset of SCO Fe(III) systems to evaluate their performance in terms of accurate calculation of the $T_{1/2}$. To the best of our knowledge, this is the first systematic work with an exclusive focus on Fe(III)-SCO systems, with the only exception of a specific study of Fe(III) quinolylsalicylaldiminate compounds, previously reported.[69] While several benchmark studies have been reported on the accuracy of different exchange-correlation functionals to predict energy differences between spin states and $T_{1/2}$ for Fe(II)-SCO systems,[52,70] no systematic study on a large dataset of Fe(III)-SCO systems has been reported yet. Given that it has already been shown that a given functional (or a given value of U in DFT+U approaches) does not result in the same accuracy when predicting spin-state energetic gaps of Fe(II) or Fe(III) systems,[45,52] it is clear that a systematic study fully devoted to Fe(III)-SCO systems is mandatory. The results of the quantitative methodology we have employed will hopefully be used in the virtual screening of new spin-crossover molecules with tailored properties, a tool that will accelerate the discovery of new members of the Fe(III) SCO family. The paper is organized as follows. First, we will present the results, followed by their discussion, and finally, the conclusions of the work.

Computational Details

All density functional calculations (DFT) have been carried out with Gaussian 16 (revision B0.1)[71] electronic structure package with a 10^{-8} convergence criterion for the density matrix elements, using the latest triple-ζ basis set with polarization functions for all elements (def2-TZVP) by Ahlrichs and co-workers.[72,73] The corresponding vibrational analysis was done for all optimized structures to ensure that they were minimums along the potential energy surface. The transition temperatures

($T_{1/2}$) were estimated by means of the following expression, which holds under the condition of thermodynamical equilibrium:

$$T_{1/2} = \frac{\Delta H_{\mathrm{HS-LS}}}{\Delta S_{\mathrm{HS-LS}}(T_{1/2})} \qquad \text{(Eq. 1)}$$

In this equation, $\Delta H_{\mathrm{HS-LS}}$ is the enthalpy difference between the HS and LS states (which is assumed to be a independent of temperature) and $\Delta S_{\mathrm{HS-LS}}$ is the entropy difference between the HS and LS states. Both $\Delta H_{\mathrm{HS-LS}}$ and $\Delta S_{\mathrm{HS-LS}}$ have an electronic and a vibrational contribution:

$$\Delta H_{\mathrm{HS-LS}} = \Delta E_{\mathrm{HS-LS}} + \Delta H_{\mathrm{vib}} \qquad \text{(Eq. 2)}$$

$$\Delta S_{\mathrm{HS-LS}}(T) = \Delta S_{\mathrm{elec}} + \Delta S_{\mathrm{vib}}(T) \qquad \text{(Eq. 3)}$$

$\Delta E_{\mathrm{HS-LS}}$ is the adiabatic energy difference between the HS and LS states. To obtain ΔS_{elec}, the electronic entropies for each state need to be evaluated, which can be done through Eq. 4:

$$S_{\mathrm{elec}} = R\ \ln(2S+1) \qquad \text{(Eq. 4)}$$

The vibrational enthalpy and entropy for each state, which are needed to evaluate ΔH_{vib} and ΔS_{vib}, can be obtained by means of the frequencies of the vibrational normal modes (ν_i) and the standard harmonic-oscillator approximations employed in statistical thermodynamics:

$$H_{\mathrm{vib}} = \sum_{i}^{N_{\mathrm{vib}}} \left(\frac{1}{2} h\nu_i + \frac{h\nu_i \mathrm{e}^{-h\nu_i/k_B T}}{1 - \mathrm{e}^{-h\nu_i/k_B T}} \right) \quad \text{(Eq. 5)}$$

$$S_{\mathrm{vib}} = \sum_{i}^{N_{\mathrm{vib}}} \left(\frac{h\nu_i}{T} \frac{1}{e^{h\nu_i/k_B T} - 1} - k_B \ln\left(1 - e^{-h\nu_i/k_B T}\right) \right) \quad \text{(Eq. 6)}$$

2. Results

To evaluate the accuracy of DFT calculations towards spin-state energy gaps in Fe^{III} spin-crossover systems, we assembled a benchmark dataset of 18 molecules, as illustrated in Figure 1. The dataset includes hexacoordinated Fe^{III} ions with different types of donor atoms sets: N_4O_2, N_3O_2Cl, $N_2O_2S_2$. For each system, we computed the energy difference between the high- and low-spin states (ΔE_{HS-LS}, Table 1) using several functionals that provided with different degrees of success when tackling the problem of spin-state energetics in SCO systems. These functionals are OPBE,[74,75] OLYP,[74,76] B3LYP,[77,78] B3LYP*,[79] TPSSh[80,81] and M06L.[82] Results are summarized in Table 1.

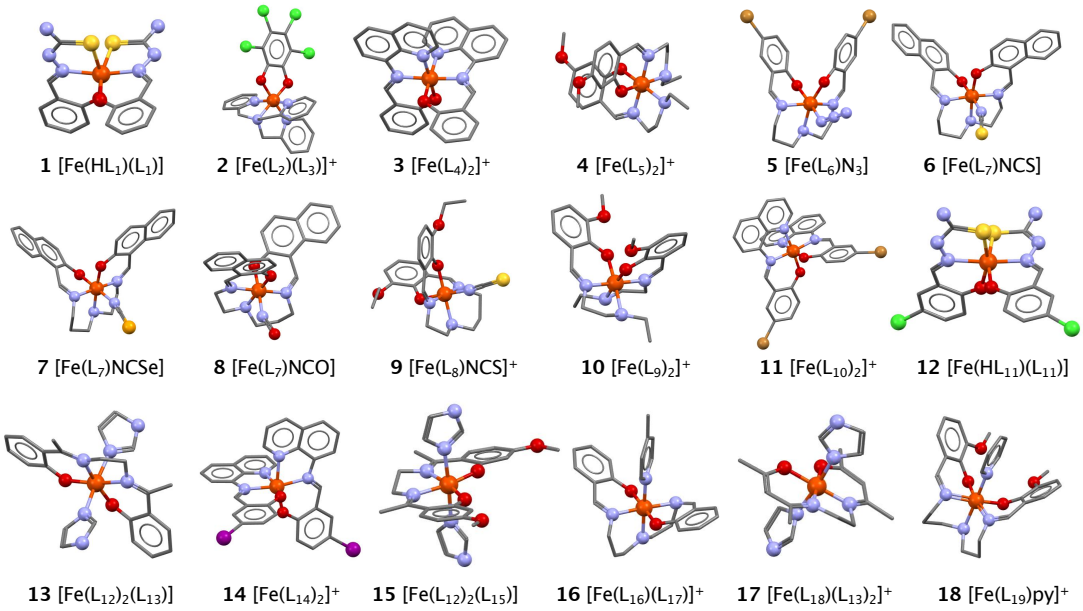

Figure 1: Schematic depiction of the studied systems in this work. H_2L_1 = salicylaldehyde thiosemicarbazone, L_2 = tris(2-Pyridylmethyl)amine-N,N',N'',N'''), L_3 = 3,4,5,6-tetrachlorocatecholato-O,O', L_4 = N-(8-quinolyl)salicylaldimine-N,N',O, L_5

= 2-(((2-(ethylamino)ethyl)imino)methyl)-5-methoxyphenolato, L_6 = N,N'-bis(2-oxy-4-bromo-benzylidene)-1,6-diamino-4-azahexane, L_7 = 1-(((3-((2-(((2-(Hydroxy)-1-naphthyl)methylene)amino)-ethyl)amino)propyl)imino)methyl)-2-naphtholato, L_8 = 2-ethoxy-6-(((3-((2-((3-ethoxy-2-(oxy)benzylidene)amino)ethyl)amino)propyl)imino)methyl)phenolato, L_9 = 2-(((2-(Ethylamino)ethyl)imino)methyl)-6-methoxyphenolato-N,N',O, L_{10} = 4-Bromo-2-(((quinolin-8-yl)imino)methyl)phenolato, H_2L_{11} = 5-chlorosalicylaldehyde thiosemicarbazone, L_{12} = 1H-imidazole, L_{13} = 2,2'-(Ethane-1,2-diylbis((nitrilo)eth-1-yl-1-ylidene))diphenolato, , L_{14} = 4-iodo-2-(((quinolin-8-yl)imino)methyl)phenolato, L_{15} = 2,2'-(ethane-1,2-diylbis((nitrilo)eth-1-yl-1-ylidene))bis(5-methoxyphenolato), H_2L_{16} = 4-azaheptamethylene-1,7-bis(salicylideneiminate), L_{17} = 4-methylpyridine, L_{18} = N,N'-Ethylene-bis(acetylacetoniminato-N,N',O,O'), L_{19} = (3-methoxysalicylideneaminopropyl)amine

Results from Table 1 can be properly visualized by plotting the average value as well as the standard deviation for the computed dataset. These results are shown in Figure 2. As can be seen in the figure, only B3LYP* and TPSSh are able to correctly predict the ground state for most systems in our dataset. This is consistent with previous benchmarks done for the TPSSh functional.[59,70] However, the most remarkable result is that B3LYP* provides with ΔE_{HS-LS} values that fit in the energy window that usually is associated with SCO to occur, this is, ΔE_{HS-LS} between 2 and 8 kcal/mol.

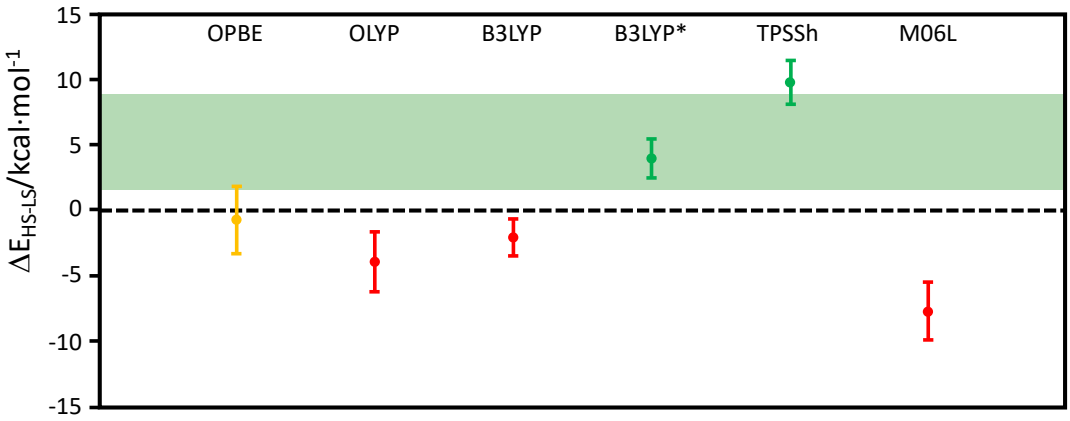

Figure 2: Average value for the spin-state energy gap (ΔE_{HS-LS}) and the corresponding standard deviation for the studied dataset using different exchange-correlation functionals. In green, the region in which spin-crossover can occur. All values in kcal·mol^{-1}.

System	*Refcode*	*OPBE*	*OLYP*	*B3LYP*	*B3LYP**	*TPSSh*	*M06L*
1	ATOJUO	2.79	-1.75	-3.59	2.24	7.96	-8.73
2	TAMTEH	0.02	-2.47	-2.82	3.67	9.32	-3.48
3	SUPHUH	2.38	-0.38	-0.39	5.98	11.32	-7.15
4	BIMZUU	-4.04	-6.17	-3.06	2.85	8.87	-8.90
5	GOWSES	-1.55	-4.14	-2.26	3.58	9.19	-9.32
6	DADFAR	-0.77	-3.81	-1.99	3.79	9.68	-9.58
7	DADFOF	-0.32	-3.43	-1.53	4.31	10.10	-9.07
8	DADGAS	-2.29	-4.91	-3.00	2.80	8.47	-10.73
9	FONNAZ	-2.15	-5.42	-3.49	2.28	8.09	-10.74
10	HAJLAH	-3.20	-5.63	-2.98	2.98	9.03	-7.92
11	PORBUV	1.99	-0.92	-0.27	5.78	11.44	-6.84
12	LIGZUY	3.19	-1.40	-3.29	2.53	8.30	-8.36
13	LIZZUR	-3.09	-6.19	-3.00	2.92	9.16	-9.02
14	XIZKEY	2.78	-0.18	-0.28	6.18	11.84	-6.73
15	XUJDOX	-3.85	-6.43	-2.37	3.45	9.50	-8.20
16	DETBEJ	-3.29	-5.80	-1.84	3.94	8.42	-5.15
17	FEWVIM	1.82	-1.21	1.42	7.61	14.13	-3.64
18	[a][Fe(L_{19})py]$^{+}$	-3.67	-6.24	-1.88	3.69	10.16	-5.63

Table 1: Spin-state energy differences (ΔE_{HS-LS} = high-spin – low-spin) for the 18 systems studied in this work. All energies include zero point corrections and are in kcal mol^{-1} . [a] No crystallographic data has been reported for system 18, and therefore no refcode can be provided.

For both functionals, an estimation of the transition temperature has been calculated using the harmonic approximation (see Computational Details). Results are summarized in Table 2.

		B3LYP*			TPSSh				
System	Refcode	ΔH	ΔS	$T_{1/2}$	ΔH	ΔS	$T_{1/2}$	$T_{1/2}$ (exp)	
1	ATOJUO	3.13	15.59	192	8.85	15.15	571	252	[83]
2	TAMTEH	4.61	13.70	336	10.24	13.00	767	232[c]	[84]
3	SUPHUH	6.84	12.84	515	12.14	12.02	979	238[c]	[85]
4	BIMZUU	3.91	14.91	248	9.91	14.40	662	152[c]	[86]
5	GOWSES	4.54	13.68	317	10.18	13.67	719	140	[87]
6	DADFAR	4.72	12.32	364	10.61	12.45	821	151	[87]
7	DADFOF	5.24	12.62	395	11.04	13.28	799	170	[87]
8	DADGAS	3.72	12.61	281	9.40	12.42	726	155	[87]
9	FONNAZ	3.20	12.71	239	9.02	12.91	671	83	[88]
10	HAJLAH	4.04	14.62	262	10.12	14.83	658	238[c]	[89]
11	PORBUV	6.588	11.60	546	12.259	11.93	997	298[b]	[90]
12	LIGZUY	3.42	15.71	208	9.21	15.81	569	231	[83]
13	LIZZUR	3.95	14.76	256	10.21	15.07	656	95[c]	[91]
14	XIZKEY	7.03	12.82	529	12.70	13.05	940	225[c]	[92]
15	XUJDOX	4.44	14.02	303	10.54	14.81	690	169[c]	[93]
16	DETBEJ	4.96	13.88	342	9.55	15.40	597	224[b]	[94]
17	FEWVIM	8.79	18.49	461	15.33	19.16	779	318[b]	[95]
18	[b][Fe(L_{19})py]$^{+}$	4.73	13.74	328	11.23	13.95	806	237[b]	[96]

Table 2: Enthalpy and entropy change for the 18 systems studied in this work using B3LYP* and TPSSh functionals, as well as the corresponding computed and

experimental values for the transition temperature ($T_{1/2}$). Enthalpies in kcal·mol^{-1}, entropies in cal·K^{-1}·mol^{-1} and temperatures in K. [b] The experimental $T_{1/2}$ has been obtained from the ΔH and ΔS measured by the Evans ^{1}H-NMR method (see Table S5 of ESI). [c] Average $T_{1/2}$ value for different counterions and co-crystallizing solvent molecules (see Table S4 of ESI)

As can be seen from Table 2, even though both functionals perform correctly in terms of predicting the ground state for all the studied systems, the computed range in energies using TPSSh is larger than with B3LYP*. This translates in much larger computed $T_{1/2}$ values when using the TPSSh functional, while B3LYP* provides with much closer values towards the experimental data.

3. Discussion

The accurate calculation of transition temperatures in SCO systems is a hard task for any computational method. However, Table 2 shows that both, TPSSh and, in a more quantitative way B3LYP* can be used to compute $T_{1/2}$ in Fe^{III}-based SCO systems. One may assume that the amount of exact exchange Hartree-Fock mixed in the functionals (10% for TPSSh and 15% for B3LYP*) is responsible for their different accuracy towards $T_{1/2}$, given that this quantity modulates the relative stability of the different spin-states. For that reason, we explored the possibility of adjusting the amount of Hartree-Fock in the B3LYP functional towards the calculation of the spin-state energy gap in Fe^{III} systems. Using S4, S6 and S11 as test cases (all of them have a sharp single step transition without hysteresis), we computed the spin state energy gap adjusting the amount of Hartree-Fock exchange mixed in the BLYP functional from 10 to 20%. Results are shown below for S6 (see ESI for S4 and S11 systems),

both for the spin-state energy gap as well as the computed $T_{1/2}$. As can be seen in Figure 3, there is a linear correlation between the amount of Hartree-Fock mixed and the spin-state energy gap. Thus, one can envision a specific *ad-hoc* functional for Fe^{III} systems. The problem is that the optimal amount of Hartree-Fock exchange mixed to reproduce the experimental temperature is different for each system, being 14%, 16% and 17% for systems S4, S6 and S11 respectively (see ESI). Thus, it seems that in order to quantitatively match the experimental values, individual reparameterizations are required, with values oscillating around the optimal 15% adjusted for B3LYP*.

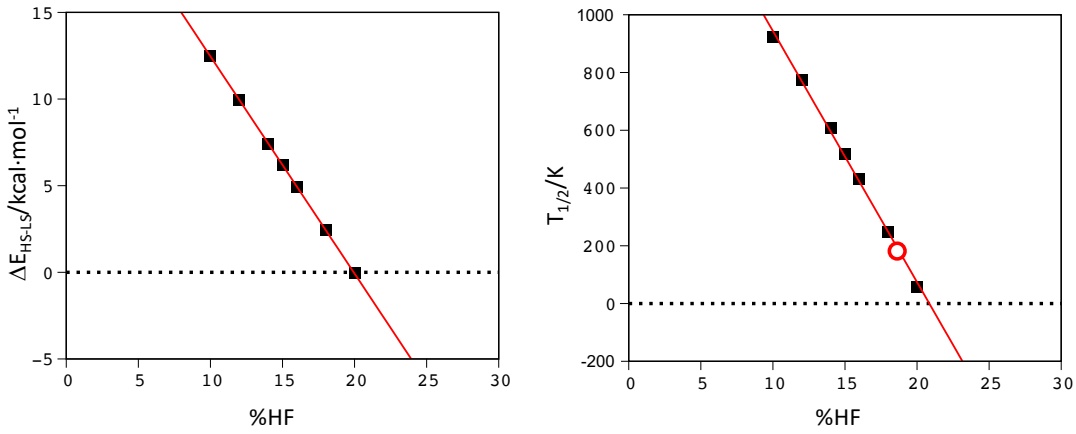

Figure 3: Computed spin-state energy (ΔE_{HS-LS}) and $T_{1/2}$ against the amount of exact exchange Hartree-Fock mixed in the BLYP functional for system S6 ([Fe(napet)NCS]). Red circle corresponds to the experimental value.

Thus, we have to assume that without any further reparameterization, B3LYP* should be a good method of choice to study Fe^{III} SCO systems. A close inspection to our dataset provides with a nice test case, formed by the family of compounds S6, S7 and S8, of general formula [Fe(napet)L] (napet = N,N'-bis(2-hydroxy-naphthylidene)-1,6-diamino-4-azahexane, L = NCS, NCSe and NCO).[87] Our calculations show increasing transition temperatures for the studied systems, this is $T_{1/2}$[Fe(napet)NCO] < $T_{1/2}$[Fe(napet)NCS] < $T_{1/2}$[Fe(napet)NCSe], in agreement with the expected trend in

the spectrochemical series. Thus, we decided to explore the applicability of the B3LYP* functional in studying the range of energies for SCO to occur, using different L ligands (L = Cl^-, N_3^-, OH^-, NCO^-, NCS^-, $NCSe^-$, NH_3 and CN^-). The computed spin-state energies and $T_{1/2}$ are shown in Table 3.

L group	f	$\Delta E_{HS\text{-}LS}$	ΔH	ΔS	$T_{1/2}$
Cl^-	0.78	3.83	2.68	10.93	246
N_3^-	0.83	5.38	4.11	14.00	294
NCO^-	0.87	4.95	3.73	12.16	307 (155)
OH^-	0.94	3.92	2.60	12.88	202
NCS^-	1.02	6.05	4.72	12.33	383 (151)
$NCSe^-$	1.03	6.53	5.18	12.67	409 (170)
NH_3	1.25	8.04	6.62	13.21	501
CN^-	1.70	14.64	13.29	13.04	1019

Table 3: Computed $\Delta E_{HS\text{-}LS}$, ΔH, ΔS and $T_{1/2}$ for the formula [Fe(napet)L] (napet = N,N'-bis(2-hydroxy-naphthylidene)-1,6-diamino-4-azahexane, L = Cl, N_3, OH, NCO, NCS, NCSe, NH_3 and CN). Energies and enthalpies in kcal mol^{-1}, entropies in $cal \cdot K^{-1} \cdot mol^{-1}$ and temperatures in K. The $T_{1/2}$ values given in brackets for NCO^-, NCS^- and $NCSe^-$ correspond to the experimental values. The *f* factor is an empirical parameter for calculating 10Dq, aiming to quantify the strength of the ligand.[97]

A plot of the computed $T_{1/2}$ against the empirical f factor for the calculation of the splitting among the d-based MOs in octahedral complexes (Figure 4) reveals a

correlation that allows us to calibrate the SCO properties of the [Fe(napet)L] systems. As can be seen, using ammonia or stronger field ligands generates a larger enough splitting of the d-based MOs to stabilize the low-spin state. This situation can be pushed even further using the cyanide ligand. Much in the same way, weaker field ligands decrease the $T_{1/2}$, and open the door for a fine-tuning degree of this property. It is thus concluded that [Fe(napet)L] provides an excellent platform for designing Fe^{III} complexes with tailored SCO properties.

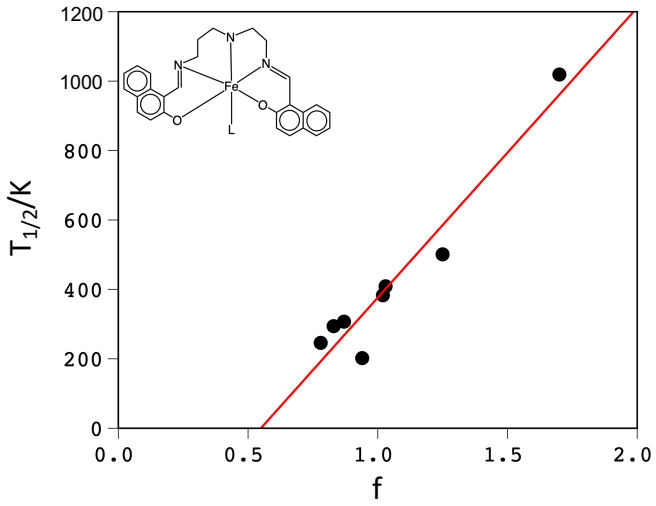

Figure 4: Computed $T_{1/2}$ for the [Fe(napet)L] (L = Cl^-, N_3^-, NCO^-, OH^-, NCS^-, $NCSe^-$, NH_3 and CN^-) systems against the f ligand factor (R^2 = 0.93).

A key difference between B3LYP* and TPSSh in terms of computing $T_{1/2}$ for Fe(III) systems is the energy window that the first one gives for SCO to occur (Figure 2). Thus, we wanted to validate the functional towards other Fe(III) systems that are either low-spin or high-spin, but do not exhibit SCO. The results are summarized in Table 4. As can be seen from the computed data, the functional provides with negative values for the spin-state energy gap for high-spin systems, and, in the case of

low-spin systems, with values that are notably larger than the ones for Fe(III) SCO systems. Thus, the functional is not only able to provide with the right energy window for SCO to occur in Fe(III) systems, but also can discriminate between high- and low-spin state systems.

System	Spin-State	ΔE_{HS-LS}	ΔH	ΔS
$[Fe(acac)_3]$	High-spin[98]	-2.63	-3.70	12.99
$[Fe(bmp)Cl_3(H_2O)]$	High-spin[99]	-17.10	-17.53	11.44
$[Fe(Cl)(L_a)]$	High-spin[100]	-3.75	-2.88	11.19
$[Fe(CN)_6]^{3-}$	Low-spin[101]	47.49	49.41	21.02
$[Fe(CN)_5(Py)]^{2-}$	Low-spin[102]	16.86	15.52	29.47
$[Fe(bipy)_3]^{3+}$	Low-spin[103]	23.56	24.56	15.42

Table 4: Computed ΔE_{HS-LS}, ΔH, ΔS for Fe(III) systems that do not exhibit SCO. Energies and enthalpies in kcal mol^{-1} and entropies in $cal \cdot K^{-1} \cdot mol^{-1}$. L_a = bis(3-salicylideneimino-propyl)amine

4. Conclusions

In this work, several DFT methods have been benchmarked towards a dataset of more than 20 different Fe(III) compounds, some exhibiting spin-crossover behavior, and others being either high- or low-spin state. From our analysis, TPSSh and B3LYP* both can correctly predict the ground state for all systems in the dataset, but B3LYP* can compute the spin-state energy gap for such systems in an energy window that allows for accurate calculation of the transition temperature in the studied systems. The overall error towards this parameter allows us to approximate the error that B3LYP* has on computing spin-state energy gaps for Fe(III) systems, which is approximately 2.00 kcal/mol (7.49 kcal/mol for TPSSh), an excellent result

for DFT calculations. Moreover, the functional can be used to study the experimentally observed trends for different members of the same family as a function of the electronic structure of the molecule. In particular, we modelled the [Fe(napet)L] family, and showed that not only we can reproduce the experimental values with great accuracy, but also we can predict the corresponding $T_{1/2}$ for other members of the same family and explain the trend on the basis of the relevant d-based molecular orbitals. Obviously, the lack of inclusion of crystal packing effects in our calculations, and the use of the lowest energy harmonic frequencies to compute the thermochemical quantities makes the quantitative agreement between computed and experimental $T_{1/2}$ a much more challenging problem. The B3LYP* functional is also able to discriminate between Fe(III) systems that do not exhibit SCO, and classify them as either high-spin or low-spin, in excellent agreement with the experimental data. The presented work thus enables the use of the B3LYP* functional to scan for new spin-crossover systems and predict, to some extent, their transition temperatures using computational tools.

Author information:

j.ribas@ub.edu

jordi.cirera@qi.ub.es

Notes: The authors declare no competing financial interest.

Acknowledgments:

J.C. thanks the Spanish MICINN for a Ramón y Cajal research contract (RYC2018-024692-I) and Spanish MICINN research grant (PID2020-115165GB-I00). J.R-A thanks the Spanish MICINN for the following research grants: CTQ2017- 87773-

P/AEI/FEDER and PID2020-117803GB-I00. J.R.-A also acknowledges financial support from the Generalitat de Catalunya (2017SGR348 grant). D. V, J.C, J.R-A thanks the Spanish Structures of Excellence María de Maeztu program (MDM-2017-0767)

Table of Contents:

A survey of different Density Functional methods for accurate calculation of spin-state energy gaps in Fe(III) complexes is reported. The data shows that the B3LYP* functional is the most accurate one in terms of predicting if a given Fe(III) system will exhibit or not spin-crossover behavior.

References:

1 P. Gütlich and H. A. Goodwin, in *Top. Curr. Chem.*, 2012, **233**, 1–47.

2 M. A. Halcrow, *Spin-Crossover Materials*, John Wiley & Sons Ltd, Oxford, UK, 2013.

3 G. Molnár, M. Mikolasek, K. Ridier, A. Fahs, W. Nicolazzi and A. Bousseksou, *Ann. Phys.*, 2019, **531**, 1900076.

4 G. Molnár, S. Rat, L. Salmon, W. Nicolazzi and A. Bousseksou, *Adv. Mater.*, 2018, **30**, 1703862.

5 G. Ke, C. Duan, F. Huang and X. Guo, *InfoMat*, 2020, **2**, 92–112.

6 M. A. Halcrow, *Dalton Trans.*, 2020, **49**, 15560–15567.

7 Z.-S. Yao, Z. Tang and J. Tao, *Chem. Commun.*, 2020, **56**, 2071–2086.

8 M. Wang, Z.-Y. Li, R. Ishikawa and M. Yamashita, *Coord. Chem. Rev.*, 2021, **435**, 213819.

9 K. S. Kumar and M. Ruben, *Angew. Chemie Int. Ed.*, 2021, **60**, 7502–7521.

10 W. Huang, X. Ma, O. Sato and D. Wu, *Chem. Soc. Rev.*, 2021, **50**, 6832–6870.

11 P. Gütlich and H. A. Goodwin, *Spin Crossover in Transition Metal Compounds III*, Springer Berlin Heidelberg, Berlin, Heidelberg, 2004, vol. 235.

12 J. Olguín, *Coord. Chem. Rev.*, 2020, **407**, 213148.

13 F. Varret, A. Bleuzen, K. Boukheddaden, A. Bousseksou, E. Codjovi, C. Enachescu, A. Goujon, J. Linares, N. Menendez and M. Verdaguer, *Pure Appl. Chem.*, 2002, **74**, 2159–2168.

14 J. A. Real, A. B. Gaspar and M. C. Muñoz, *Dalton Trans.*, 2005, 2062.

15 M. A. Halcrow, *Chem. Soc. Rev.*, 2011, **40**, 4119.

16 S. Brooker, *Chem. Soc. Rev.*, 2015, **44**, 2880–2892.

17 O. Sato, *Nat. Chem.*, 2016, **8**, 644–656.

18 K. Senthil Kumar and M. Ruben, *Coord. Chem. Rev.*, 2017, **346**, 176–205.

19 P. Gütlich, A. B. Gaspar and Y. Garcia, *Beilstein J. Org. Chem.*, 2013, **9**, 342–391.

20 H. Paulsen, V. Schünemann and J. A. Wolny, *Eur. J. Inorg. Chem.*, 2013, **2013**, 628–641.

21 L. Cambi and L. Szegö, *Berichte der Dtsch. Chem. Gesellschaft (A B Ser.*, 1931, **64**, 2591–2598.

22 P. Gütlich, *Eur. J. Inorg. Chem.*, 2013, **2013**, 581–591.

23 P. Gütlich, Y. Garcia and H. A. Goodwin, *Chem. Soc. Rev.*, 2000, **29**, 419–427.

24 H. A. Goodwin, in *Top. Curr. Chem.*, 2012, **233**, 59–90.

25 M. A. Halcrow, *Polyhedron*, 2007, **26**, 3523–3576.

26 J. Olguín and S. Brooker, *Coord. Chem. Rev.*, 2011, **255**, 203–240.

27 G. Aromí, L. A. Barrios, O. Roubeau and P. Gamez, *Coord. Chem. Rev.*, 2011, **255**, 485–546.

28 G. A. Craig, O. Roubeau and G. Aromí, *Coord. Chem. Rev.*, 2014, **269**, 13–31.

29 H. L. C. Feltham, A. S. Barltrop and S. Brooker, *Coord. Chem. Rev.*, 2017, **344**, 26–53.

30 H. S. Scott, R. W. Staniland and P. E. Kruger, *Coord. Chem. Rev.*, 2018, **362**, 24–43.

31 T. Gebretsadik, Q. Yang, J. Wu and J. Tang, *Coord. Chem. Rev.*, 2021, **431**, 213666.

32 P. J. Koningsbruggen, Y. Maeda and H. Oshio, in *Top. Curr. Chem.*, **233**, 2012, 259–324.

33 M. Nihei, T. Shiga, Y. Maeda and H. Oshio, *Coord. Chem. Rev.*, 2007, **251**, 2606–2621.

34 D. J. Harding, P. Harding and W. Phonsri, *Coord. Chem. Rev.*, 2016, **313**, 38–61.

35 M. Nakaya, R. Ohtani, L. F. Lindoy and S. Hayami, *Inorg. Chem. Front.*, 2021, **8**, 484–498.

36 M. Reiher, *Inorg. Chem.*, 2002, **41**, 6928–6935.

37 A. Rudavskyi, C. Sousa, C. de Graaf, R. W. A. Havenith and R. Broer, *J. Chem. Phys.*, 2014, **140**, 184318.

38 S. R. Mortensen and K. P. Kepp, *J. Phys. Chem. A*, 2015, **119**, 4041–4050.

39 S. Vela, M. Fumanal, J. Ribas-Arino and V. Robert, *Phys. Chem. Chem. Phys.*,

2015, **17**, 16306–16314.

40 E. I. Ioannidis and H. J. Kulik, *J. Chem. Phys.*, 2015, **143**, 034104.

41 M. Fumanal, L. K. Wagner, S. Sanvito and A. Droghetti, *J. Chem. Theory Comput.*, 2016, **12**, 4233–4241.

42 K. P. Kepp, *Inorg. Chem.*, 2016, **55**, 2717–2727.

43 L. Wilbraham, P. Verma, D. G. Truhlar, L. Gagliardi and I. Ciofini, *J. Phys. Chem. Lett.*, 2017, **8**, 2026–2030.

44 J. P. Janet and H. J. Kulik, *Chem. Sci.*, 2017, **8**, 5137–5152.

45 O. S. Siig and K. P. Kepp, *J. Phys. Chem. A*, 2018, **122**, 4208–4217.

46 S. Song, M.-C. Kim, E. Sim, A. Benali, O. Heinonen and K. Burke, *J. Chem. Theory Comput.*, 2018, **14**, 2304–2311.

47 H. Paulsen and A. X. Trautwein, *J. Phys. Chem. Solids*, 2004, **65**, 793–798.

48 Q. M. Phung, M. Feldt, J. N. Harvey and K. Pierloot, *J. Chem. Theory Comput.*, 2018, **14**, 2446–2455.

49 G. Prokopiou and L. Kronik, *Chem. - A Eur. J.*, 2018, **24**, 5173–5182.

50 M. Radoń, *Phys. Chem. Chem. Phys.*, 2019, **21**, 4854–4870.

51 A. Römer, L. Hasecke, P. Blöchl and R. A. Mata, *Molecules*, 2020, **25**, 5176.

52 S. Vela, M. Fumanal, J. Cirera and J. Ribas-Arino, *Phys. Chem. Chem. Phys.*, 2020, **22**, 4938–4945.

53 L. A. Mariano, B. Vlaisavljevich and R. Poloni, *J. Chem. Theory Comput.*, 2021, **17**, 2807–2816.

54 D. C. Ashley and E. Jakubikova, *Coord. Chem. Rev.*, 2017.

55 J. Nance, D. N. Bowman, S. Mukherjee, C. T. Kelley and E. Jakubikova, *Inorg. Chem.*, 2015, **54**, 11259–11268.

56 A. Fouqueau, M. E. Casida, L. M. L. Daku, A. Hauser and F. Neese, *J. Chem.*

Phys., 2005, **122**, 044110.

57 M. Swart, *J. Chem. Theory Comput.*, 2008, **4**, 2057–2066.

58 S. Lebègue, S. Pillet and J. G. Ángyán, *Phys. Rev. B*, 2008, **78**, 024433.

59 K. P. Jensen and J. Cirera, *J. Phys. Chem. A*, 2009, **113**, 10033–10039.

60 M. Kepenekian, V. Robert, B. Le Guennic and C. De Graaf, *J. Comput. Chem.*, 2009, **30**, 2327–33.

61 A. Domingo, M. Àngels Carvajal and C. de Graaf, *Int. J. Quantum Chem.*, 2010, **110**, 331–337.

62 T. Bučko, J. Hafner, S. Lebègue and J. G. Ángyán, *Phys. Chem. Chem. Phys.*, 2012, **14**, 5389.

63 J. Cirera and F. Paesani, *Inorg. Chem.*, 2012, **51**, 8194–8201.

64 J. Cirera and E. Ruiz, *J. Mater. Chem. C*, 2015, **3**, 7954–7961.

65 J. Cirera and E. Ruiz, *Inorg. Chem.*, 2016, **55**, 1657–1663.

66 J. Cirera and E. Ruiz, *Comments Inorg. Chem.*, 2019, **39**, 216–241.

67 J. Cirera and E. Ruiz, *Inorg. Chem.*, 2018, **57**, 702–709.

68 L. Navarro, F. Rodriguez and J. Cirera, *Dalton Trans.*, 2021, **50**, 8704–8710.

69 J. Sirirak, D. Sertphon, W. Phonsri, P. Harding and D. J. Harding, *Int. J. Quantum Chem.*, 2017, **117**, e25362.

70 J. Cirera, M. Via-Nadal and E. Ruiz, *Inorg. Chem.*, 2018, **57**, 14097–14105.

71 M. J. Frisch, G. W. Trucks, H. B. Schlegel, G. E. Scuseria, M. A. Robb, J. R. Cheeseman, G. Scalmani, V. Barone, G. A. Petersson, H. Nakatsuji, X. Li, M. Caricato, A. V. Marenich, J. Bloino, B. G. Janesko, R. Gomperts, B. Mennucci, H. P. Hratchian, J. V. Ortiz, A. F. Izmaylov, J. L. Sonnenberg, D. Williams-Young, F. Ding, F. Lipparini, F. Egidi, J. Goings, B. Peng, A. Petrone, T. Henderson, D. Ranasinghe, V. G. Zakrzewski, J. Gao, N. Rega, G. Zheng, W.

Liang, M. Hada, M. Ehara, K. Toyota, R. Fukuda, J. Hasegawa, M. Ishida, T. Nakajima, Y. Honda, O. Kitao, H. Nakai, T. Vreven, K. Throssell, J. Montgomery, J. A., J. E. Peralta, F. Ogliaro, M. J. Bearpark, J. J. Heyd, E. N. Brothers, K. N. Kudin, V. N. Staroverov, T. A. Keith, R. Kobayashi, J. Normand, K. Raghavachari, A. P. Rendell, J. C. Burant, S. S. Iyengar, J. Tomasi, M. Cossi, J. M. Millam, M. Klene, C. Adamo, R. Cammi, J. W. Ochterski, R. L. Martin, K. Morokuma, O. Farkas, J. B. Foresman and D. J. Fox, *Gaussian, Inc., Wallingford, CT*.

72 F. Weigend and R. Ahlrichs, *Phys. Chem. Chem. Phys.*, 2005, **7**, 3297–3305.

73 F. Weigend, *Phys. Chem. Chem. Phys.*, 2006, **8**, 1057–1065.

74 N. C. Handy and A. J. Cohen, *Mol. Phys.*, 2001, **99**, 403–412.

75 J. P. Perdew, K. Burke and M. Ernzerhof, *Phys. Rev. Lett.*, 1997, **78**, 1396.

76 C. Lee, W. Yang and R. G. Parr, *Phys. Rev. B*, 1988, **37**, 785–789.

77 A. D. Becke, *J. Chem. Phys.*, 1993, **98**, 5648–5652.

78 P. J. Stephens, F. J. Devlin, C. F. Chabalowski and M. J. Frisch, *J. Phys. Chem.*, 1994, **98**, 11623–11627.

79 O. Salomon, M. Reiher and B. A. Hess, *J. Chem. Phys.*, 2002, **117**, 4729–4737.

80 J. Tao, J. P. Perdew, V. N. Staroverov and G. E. Scuseria, *Phys. Rev. Lett.*, 2003, **91**, 146401.

81 J. P. Perdew, J. Tao, V. N. Staroverov and G. E. Scuseria, *J. Chem. Phys.*, 2004, **120**, 6898–6911.

82 Y. Zhao and D. G. Truhlar, *J. Chem. Phys.*, 2006, **125**, 194101.

83 E. W. T. Yemeli, G. R. Blake, A. P. Douvalis, T. Bakas, G. O. R. Alberda van Ekenstein and P. J. Koningsbruggen, *Chem. – A Eur. J.*, 2019, **25**, 16766–16776.

84 E. Collet, M.-L. Boillot, J. Hebert, N. Moisan, M. Servol, M. Lorenc, L. Toupet, M. Buron-Le Cointe, A. Tissot and J. Sainton, *Acta Crystallogr. Sect. B Struct. Sci.*, 2009, **65**, 474–480.

85 K. Takahashi, H. Mori, H. Kobayashi and O. Sato, *Polyhedron*, 2009, **28**, 1776–1781.

86 A. Tissot, P. Fertey, R. Guillot, V. Briois and M.-L. Boillot, *Eur. J. Inorg. Chem.*, 2014, **2014**, 101–109.

87 I. Nemec, R. Herchel, R. Boča, Z. Trávníček, I. Svoboda, H. Fuess and W. Linert, *Dalton Trans.*, 2011, **40**, 10090–10099.

88 P. Masárová, P. Zoufalý, J. Moncol, I. Nemec, J. Pavlik, M. Gembický, Z. Trávníček, R. Boča and I. Šalitroš, *New J. Chem.*, 2015, **39**, 508–519.

89 A. Tissot, R. Bertoni, E. Collet, L. Toupet and M.-L. Boillot, *J. Mater. Chem.*, 2011, **21**, 18347.

90 W. Phonsri, D. J. Harding, P. Harding, K. S. Murray, B. Moubaraki, I. A. Gass, J. D. Cashion, G. N. L. Jameson and H. Adams, *Dalton Trans.*, 2014, **43**, 17509–17518.

91 T. Fujinami, M. Koike, N. Matsumoto, Y. Sunatsuki, A. Okazawa and N. Kojima, *Inorg. Chem.*, 2014, **53**, 2254–2259.

92 K. Fukuroi, K. Takahashi, T. Mochida, T. Sakurai, H. Ohta, T. Yamamoto, Y. Einaga and H. Mori, *Angew. Chemie Int. Ed.*, 2014, **53**, 1983–1986.

93 T. Fujinami, M. Ikeda, M. Koike, N. Matsumoto, T. Oishi and Y. Sunatsuki, *Inorganica Chim. Acta*, 2015, **432**, 89–95.

94 N. Matsumoto, S. Ohta, C. Yoshimura, A. Ohyoshi, S. Kohata, H. Okawa and Y. Maeda, *J. Chem. Soc., Dalton Trans.*, 1985, 2575.

95 Y. Nishida, K. Kino and S. Kida, *J. Chem. Soc., Dalton Trans.*, 1987, 1157.

96 A. Ohyoshi, J. Honbo, N. Matsumoto, S. Ohta and S. Sakamoto, *Bull. Chem. Soc. Jpn.*, 1986, **59**, 1611–1613.

97 C. K. Jørgensen, *Modern aspects of ligand field theory*, 1971.

98 G. M. Bancroft, A. G. Maddock, W. K. Ong, R. H. Prince and A. J. Stone, *J. Chem. Soc. A*, 1967, 1966–1971.

99 G. De Munno, W. Ventura, G. Viau, F. Lloret, J. Faus and M. Julve, *Inorg. Chem.*, 1998, **37**, 1458–1464.

100 M. Y. Volkov, E. N. Frolova, L. V. Mingalieva, L. G. Gafiyatullin, O. A. Turanova, E. O. Milordova, I. V. Ovchinnikov and A. N. Turanov, *Polyhedron*, 2018, **154**, 407–410.

101 *Modern Coordination Chemistry Edited by J. Lewis and R. G. Wilkins. Pp. xvi + 487. Interscience Publishers Inc., New York; Interscience Publishers Ltd, London. 1960. 80s. net*, 1960, vol. 19.

102 G. M. Chiarella, D. Y. Melgarejo and S. A. Koch, *J. Am. Chem. Soc.*, 2006, **128**, 1416–1417.

103 B. Figgis, B. Skelton and A. White, *Aust. J. Chem.*, 1978, **31**, 57.